International Refereed Journal of Engineering and Science (IRJES)
ISSN (Online) 2319-183X, (Print) 2319-1821
Volume 7, Issue 6 Ver. I (Jun 2018), PP. 45-62

Ultra-broadband 4×4 and 8×8 Butler Beam Forming Networks on Liquid Crystal Substrate at 51Ghz

Abdullah H. Alhazmi, Adnan Affandi
King Abdullaziz University

Abstract: *The main objective of this proposed work is to improve the performances of the individual components which are forming the butler beam forming networks. The second objective is to implement all these proposed. Butler matrices on Liquid Crystal substrate (50-60 GHz). The third objective is to develop unique signal flow (S, G, F) for both 4×4 and 8×8 butler matrices in order to compute their scattering matrices at the operating frequency. All the butler networks are subjected to optimization procedure. An enhancement factor will be applied in order to improve the gains of some of selected patch antennas inform of signals and arrays. Converting the linear radiation of the single and array into circular ones will fully demonstrate in this work.*

Keywords: *Butler matrix for microstrip, for beam forming network.*

Date of Submission:31-08-2018 Date of acceptance: 15-09-2018

I. Introduction

One of the most widely known of switched beam forming networks is butler matrix. If N×N positive feeding network with beam steering capabilities for phase array antennas with N outputs and N inputs feeding an N-element antenna array using N×N butler matrix, N orthogonal beams can be generator, each beam has again of the whole array [1-10].

It is well known fact that 1×4, 4×4, 4×8, 8×8 and 16×16 butlers matrices are composed of several elements which are informing the butler matrices. These elements are one section (Branch line couplers or sometime Lange couplers), two sections Branch line couplers (known as the crossover) and phase shifters [1-10].

Once the proper patch antennas inform of singles or arrays are connected to the selected butler matrices to form what is known as the butler beam forming networks.

1.1. The One and Two Sections Branch Line Couplers

Simple signal flow (SGF) are developed in order to compute the scattering matrices of the one and two sections branch line couples at the central frequency are illustrated below:

1.1.1. The One Section Branch Line Coupler

The Signal Flow of the One-section Branch Line Coupler with its derived scattering matrix is shown below:

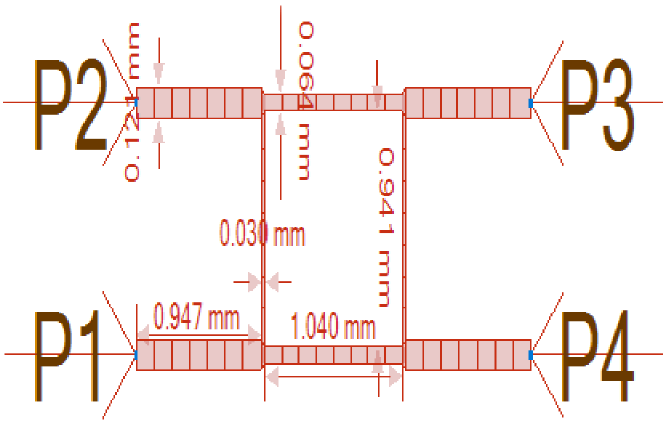

Figure 1.1 Shows the layout of one section branch line coupler

- The signal flow of One Section branch line coupler is drawn below:

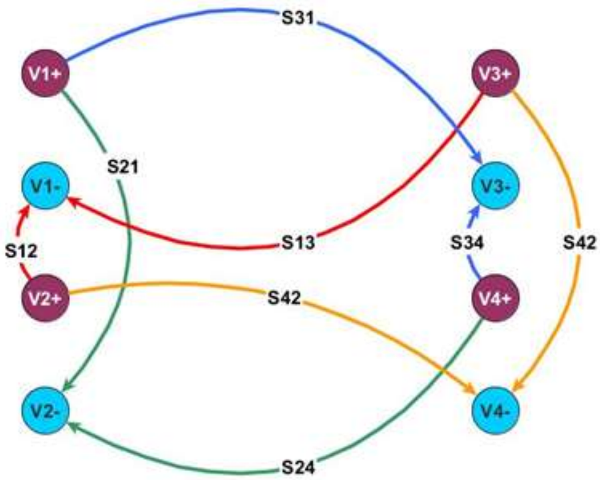

Figure 1.2 Show the Signal Flow of 4-Port Branch Coupler

The computed scattering matrix for one section branch line coupler

$$S = \frac{-1}{\sqrt{2}} \begin{bmatrix} 0 & j & 1 & 0 \\ j & 0 & 0 & 1 \\ 1 & 0 & 0 & j \\ 0 & 1 & j & 0 \end{bmatrix} \qquad 1.1$$

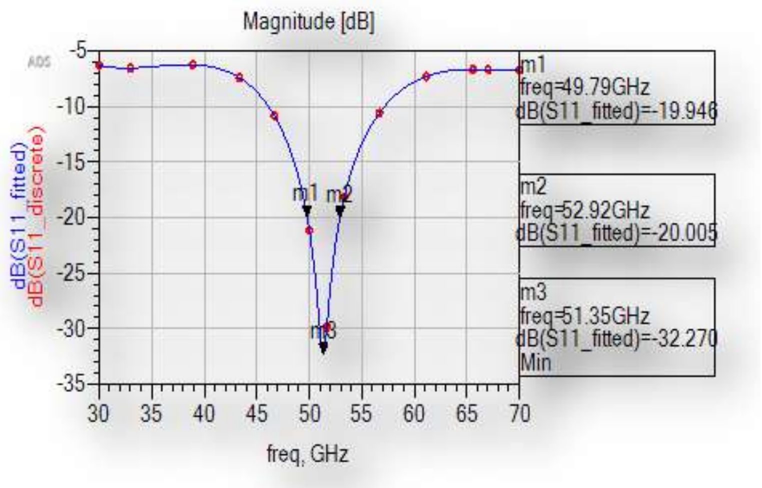

Figure 1.3 The Simulated return loss of the 90° hybrid coupler as function of frequency

Table 1.1 Summarize the Simulated Result of the One Section Branch Line Coupler

Center Frequency (F_c)	50.08 GHz
Bandwidth (GHz)	Hz

1.1.2. The Two Sections Branch Line Coupler

The Signal Flow (S.G.F) for the Two Sections Branch Line Coupler with its Scattering Matrix at the Central Frequency is given below:

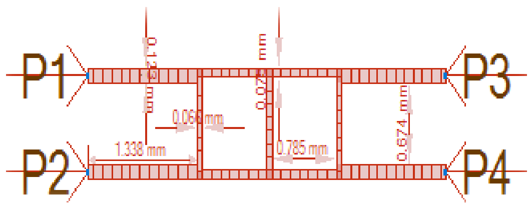

Figure 1.4 Depicts the Two Section Branch Coupler

The derived Scattering matrix for 0dB crossover branch line coupler list below:

$$S = \begin{bmatrix} 0 & 0 & j & 0 \\ 0 & 0 & 0 & j \\ j & 0 & 0 & 0 \\ 0 & j & 0 & 0 \end{bmatrix} \qquad 1.2$$

- The signal flow of the 2-Section Branch line Coupler is drawn below:

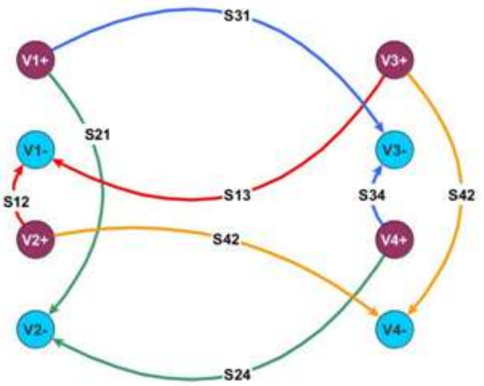

Figure 1.5 Signal Flow of 2-Section for 4-Port Branch line Coupler

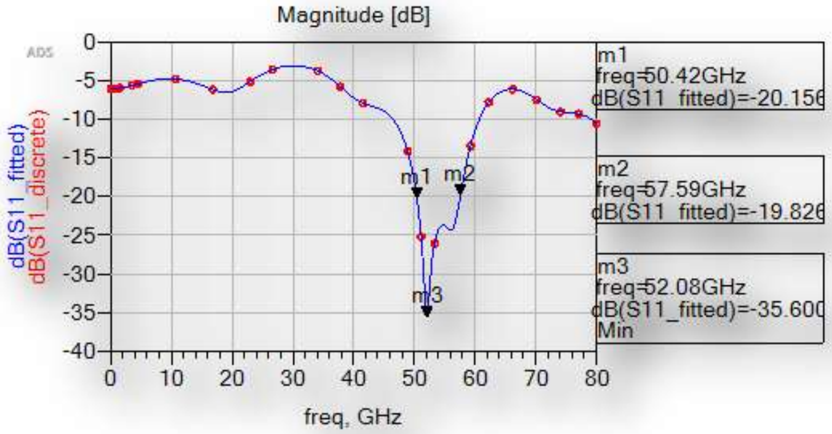

Figure 1.6 The Return Loss of The Two Section Shows Branch Line Coupler on Liquid Crystal Substrate at the Central Frequency of 50.08GHz and Bandwidth of 7.17GHz

The computed bandwidth is bandwidth is given in table (1.2)

TABLE 1.2 List Both the (Central Frequency and the Computed Bandwidth)

Center Frequency (F_c)	51.35 GHz
Bandwidth (GHz)	Hz

1.1.3. The Improved Two Port Microstrip Phase Shifter

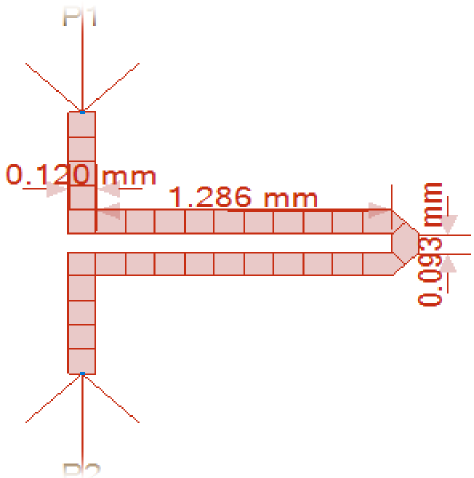

Figure 1.7 Depicts the Layout of the Microstrip Phase Shifter

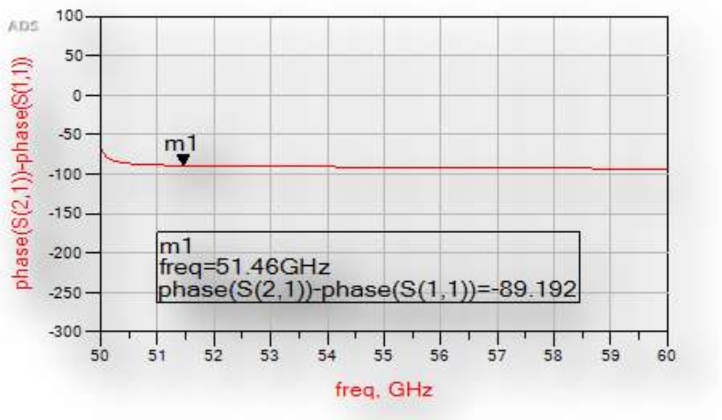

Figure 1.8 Shows the Simulated Phase Shifter as Function Frequency

Table 1.3 Summarize the phase Shifter Performance

Center Frequency (F_c)	51.35 GHz
Bandwidth (GHz)	3.13 GHz
Phase (S21-S11)	89.192

II. Construction of Butler Matrix

2.1. Layout Butler Matrix 4×4

Figure 2.1 shows the block structure and layout of the Butler Matrix While its simulated response as a function of frequency is shown in Fig 2.2. The Butler Matrix has four inputs 1R, 2L, 2R and 1L, and four outputs A1, A2, A3 and A4. The four outputs are used as inputs to antenna elements to produce four beams. Four hybrid couplers, two crossovers, two phase shifter (45) were combined to produce the Butler Matrix.

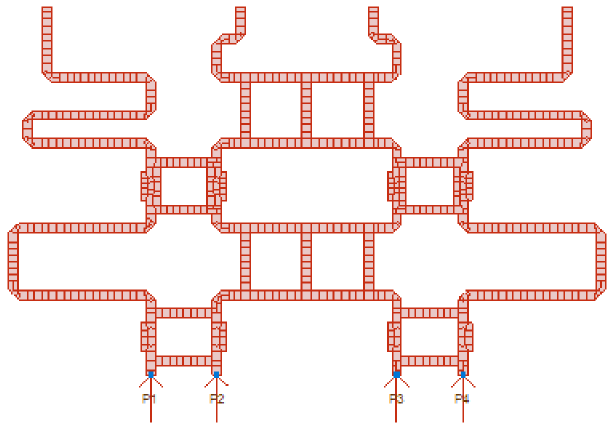

(a)

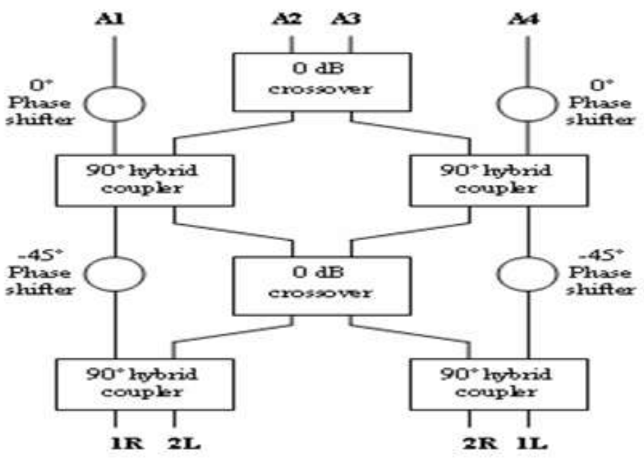

(b)

Figure 2.1 Butler Matrix configuration (a) The layout (b) The block structure

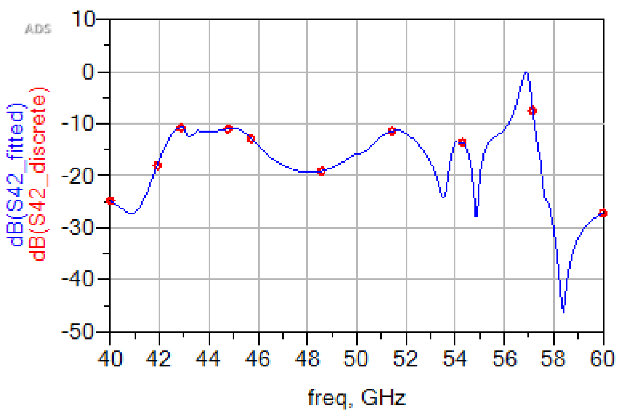

Figure 2.2 Shows the Return Loss of 4×4 Butler Matrix

2.2. Layout of 8×8 Butler Matrix

Figure 2.3 shows the layout of the Butler Matrix While its simulated response as a function of frequency is shown in Fig 2.4.

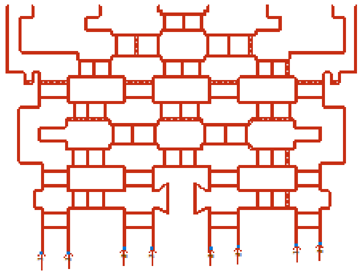

Figure 2.3 Shows the Layout of Butler Matrix configuration

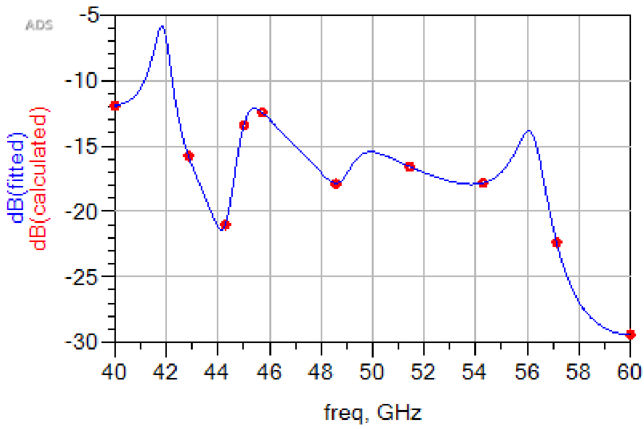

Figure 2.4 The Simulated Return Loss of the Butler Matrix

III. The Methodology to Design Array Patch Antenna

Selections of several types of patch antennas of different shapes and configurations are designed, simulated and optimized for operation on liquid crystal substrate. The most suitable selected antenna for 4×4 and 8×8 butler matrices is found to be the rectangular shape cut at the corner with slot generated at the ground plane.

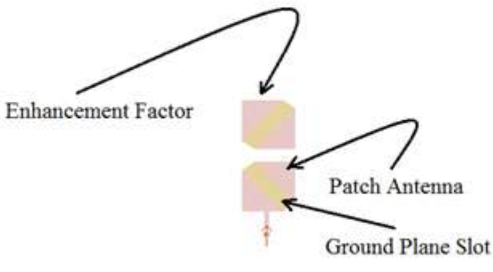

Figure 3.1 Depicts the layout of two rectangular shape cut at the corners with the generated slot in the ground plane

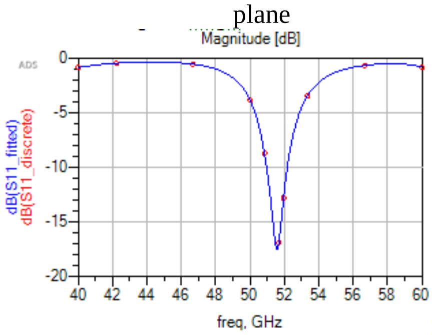

plane

Figure 3.2 Shows the Return Loss of Figure (3.1) of the Single Microstrip Rectangular Shaped Patch Antenna Cut at the Corners with the Generated Ground Plane Slot and Enhancement Factor

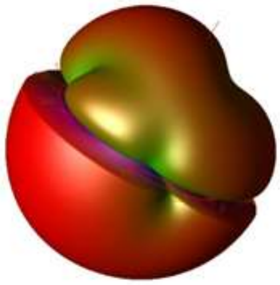

Figure 3.3 Depicts the 3D Radiation Pattern of the Single Microstrip Rectangular Patch Antenna

2.3. The 4x4 Butler Matrix Analysis by Using the Developed Signal Flow

An unique signal flow technique is developed in order to compute the scattering of 4×4 butler matrix at the central frequency is shown at three trials below.

- The Signal Flow of the 4×4 Butler Matrix with Microstrip Rectangular-cut at the Corners

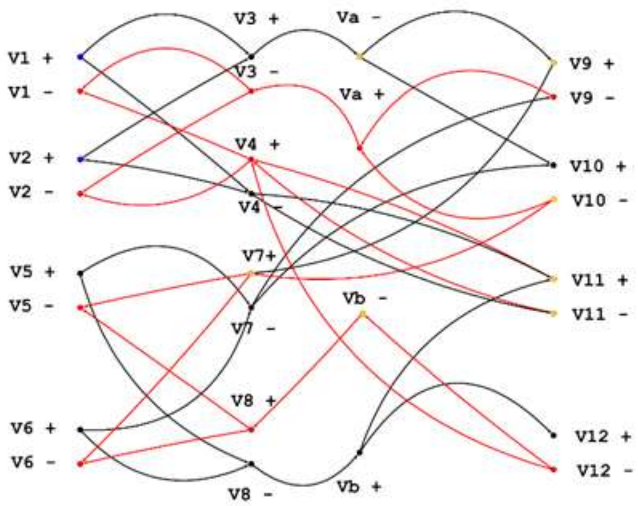

- Using the developed signal flow to compute the 4×4 butler scarring matrix at the central frequency

$$S = \frac{-1}{\sqrt{2}}\begin{bmatrix} 0 & 0 & 0 & 0 & \angle 135^{o} & \angle 45^{o} & \angle 90^{o} & \angle 0^{o} \\ 0 & 0 & 0 & 0 & \angle 45^{o} & \angle 135^{o} & \angle 90^{o} & \angle 0^{o} \\ 0 & 0 & 0 & 0 & \angle 90^{o} & \angle 0^{o} & \angle 45^{o} & \angle 135^{o} \\ 0 & 0 & 0 & 0 & \angle 0^{o} & \angle 90^{o} & \angle 135^{o} & \angle 45^{o} \\ \angle 135^{o} & \angle 45^{o} & \angle 90^{o} & \angle 0^{o} & 0 & 0 & 0 & 0 \\ \angle 45^{o} & \angle 135^{o} & \angle 0^{o} & \angle 90^{o} & 0 & 0 & 0 & 0 \\ \angle 90^{o} & \angle 0^{o} & \angle 45^{o} & \angle 135^{o} & 0 & 0 & 0 & 0 \\ \angle 0^{o} & \angle 90^{o} & \angle 135^{o} & \angle 45^{o} & 0 & 0 & 0 & 0 \end{bmatrix}$$

Table 3.1 Substrate Parameters

Substrate	LiquidCrystal
Dielectric Constant □ r	3.2
Substrate Height	m

2.3.1. <u>1st Trail</u> " 4x4 Butler Matrix with Rectangular Parallelepiped Shaped Patch Antennas ".

The layout of the simulation and optimization of 4×4 butler beamforming network:

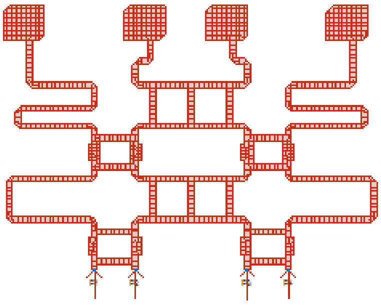

Figure 3.4 4x4 Butler matrix with Rectangular Parallelepiped shaped patch antennas

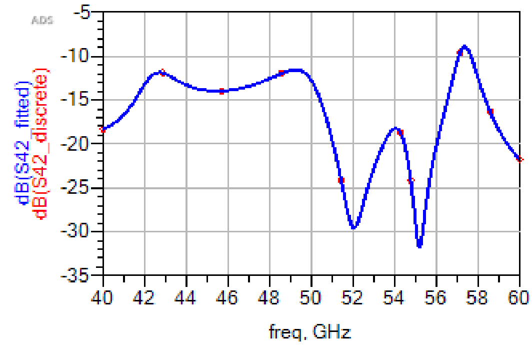

Figure 3.5 Shows the Return Loss of the 4x4 Butler matrix with Rectangular Parallelepiped-ped Shaped Patch Antenna

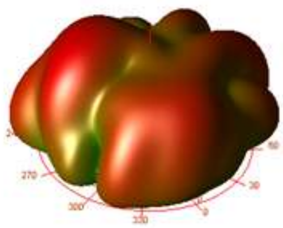

Figure 3.6 3D Radiation pattern of the 4x4 Butler Matrix with Rectangular Parallelepiped Shaped Patch Antenna

Table 3.2 Antenna Parameters of 4x4 Butler Matrix with Rectangular Parallelepiped Shaped Patch Antenna

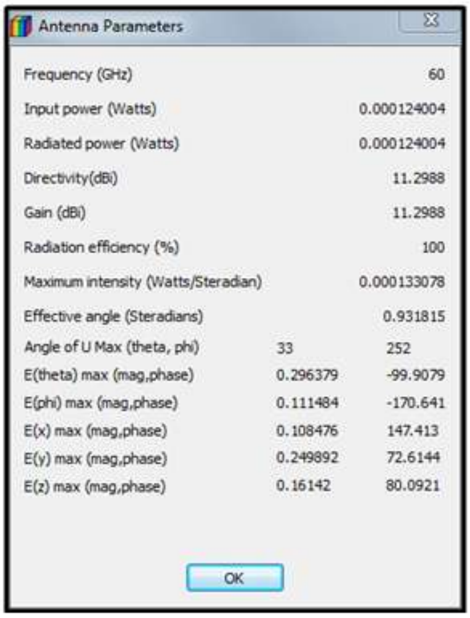
Antenna Parameters

Frequency (GHz)		60
Input power (Watts)		0.000124004
Radiated power (Watts)		0.000124004
Directivity(dBi)		11.2988
Gain (dBi)		11.2988
Radiation efficiency (%)		100
Maximum intensity (Watts/Steradian)		0.000133078
Effective angle (Steradians)		0.931815
Angle of U Max (theta, phi)	33	252
E(theta) max (mag,phase)	0.296379	-99.9079
E(phi) max (mag,phase)	0.111484	-170.641
E(x) max (mag,phase)	0.108476	147.413
E(y) max (mag,phase)	0.249892	72.6144
E(z) max (mag,phase)	0.16142	80.0921

OK

2.3.2. <u>2nd Trail</u> " 4x4 Butler Matrix with Rectangular Parallelepiped Shaped Patch Antennas with the Generated Ground Plane Slot".

The layout of the simulate and optimized 4×4 butler beamforming network.

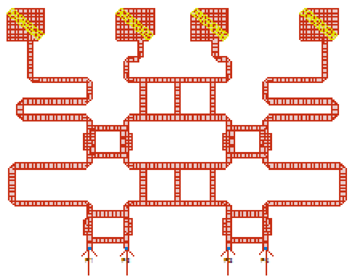

Figure 3.7 4x4 Butler matrix with Rectangular Parallelepiped shaped patch antennas with Slot

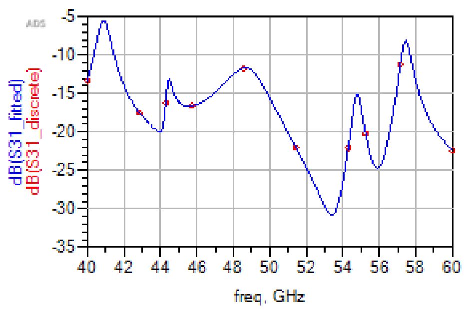

Figure 3.8 Shows the Return Loss of the 4x4 Butler matrix with Rectangular Parallelepiped-ped Shaped Patch Antenna with Slot.

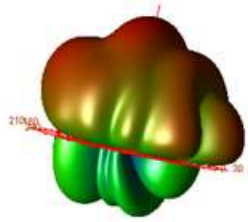

Figure 3.9 3D Radiation pattern of the 4x4 Butler Matrix with Rectangular Parallelepiped Shaped Patch Antenna with Slot

Table 3.3 Antenna Parameters of 4x4 Butler Matrix with Rectangular Parallelepiped Shaped Patch Antenna with Slot

Antenna Parameters		
Frequency (GHz)		51.4286
Input power (Watts)		0.00122551
Radiated power (Watts)		0.00107888
Directivity(dBi)		11.9748
Gain (dBi)		11.4213
Radiation efficiency (%)		88.035
Maximum intensity (Watts/Steradian)		0.00135282
Effective angle (Steradians)		0.797503
Angle of U Max (theta, phi)	2	143
E(theta) max (mag,phase)	0.769679	-16.9375
E(phi) max (mag,phase)	0.653372	-167.912
E(x) max (mag,phase)	0.331011	127.866
E(y) max (mag,phase)	0.95342	-1.53774
E(z) max (mag,phase)	0.0268614	163.062

2.3.3. <u>The Final Trail (The required Improved shape)</u>" 4x4 Butler Matrix with Rectangular Parallelepiped Shaped Patch Antennas with Slot and Enhancement Factor ".

The layout of the simulate and optimized 4×4 butler beamforming network.

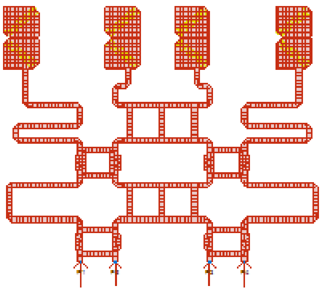

Figure 3.10 4x4 Butler Matrix with Rectangular Parallelepiped Shaped Patch Antennas with Slot and Enhancement Factor

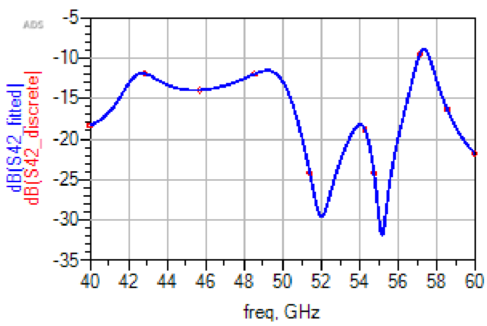

Figure 3.11 Shows the Return Loss of the 4x4 Butler Matrix with Rectangular Parallelepiped-ped Shaped Patch Antenna with Slot and Enhancement Factor

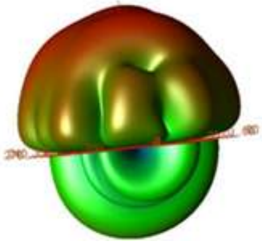

Figure 3.12 3D Radiation pattern of the 4x4 Butler Matrix with Rectangular Parallelepiped Shaped Patch Antenna with Slot and Enhancement Factor

Table 3.4 Antenna Parameters of 4x4 Butler Matrix with Rectangular Parallelepiped Shaped Patch Antenna

Frequency (GHz)		51.4286
Input power (Watts)		0.00102687
Radiated power (Watts)		0.000963161
Directivity(dBi)		12.5143
Gain (dBi)		12.2362
Radiation efficiency (%)		93.7959
Maximum intensity (Watts/Steradian)		0.00136748
Effective angle (Steradians)		0.704333
Angle of U Max (theta, phi)	17	158
E(theta) max (mag,phase)	0.906045	47.5334
E(phi) max (mag,phase)	0.457629	-179.343
E(x) max (mag,phase)	0.697492	-122.132
E(y) max (mag,phase)	0.688239	20.7911
E(z) max (mag,phase)	0.264902	-132.467
OK		

❖ It is clear from figure 3.12 that the 3D radiation pattern obtained is acceptable according to the design requirement which required circular polarized operation.

2.4. The 8x8 Butler Matrix Analysis by Using the Developed Signal Flow

An unique signal flow technique is developed in order to compute the scattering of 8×8 butler matrix at the central frequency is shown below.

The scattering matrix for 8x8 Butler Matrix with Rectangular-cut at the corners Shaped Patch Antennas

$$S = \left[\begin{array}{cccccccccccccccc}
0 & 0 & 0 & 0 & 0 & 0 & 0 & 0 & .35\angle -157^{0} & .35\angle 112.5^{0} & .35\angle 45^{0} & .35\angle 45^{0} & .35\angle 112.5^{0} & .35\angle 22.5^{0} & .35\angle -90^{0} & .35\angle 0^{0} \\
0 & 0 & 0 & 0 & 0 & 0 & 0 & 0 & .35\angle 112.5^{0} & .35\angle 22.5^{0} & .35\angle -225^{0} & .35\angle -135^{0} & .35\angle -22.5^{0} & .35\angle -112.5^{0} & .35\angle 0^{0} & .35\angle -90^{0} \\
0 & 0 & 0 & 0 & 0 & 0 & 0 & 0 & .35\angle 45^{0} & .35\angle -45^{0} & .35\angle -22.5^{0} & .35\angle -112.5^{0} & .35\angle 90^{0} & .35\angle 0^{0} & .35\angle -22.5^{0} & .35\angle 292.5^{0} \\
0 & 0 & 0 & 0 & 0 & 0 & 0 & 0 & .35\angle -45^{0} & .35\angle -139^{0} & .35\angle -229^{0} & .35\angle 22.5^{0} & .35\angle 0^{0} & .35\angle -90^{0} & .35\angle 112.5^{0} & .35\angle 22.5^{0} \\
0 & 0 & 0 & 0 & 0 & 0 & 0 & 0 & .35\angle 22.5^{0} & .35\angle 112.5^{0} & .35\angle -90^{0} & .35\angle 0^{0} & .35\angle 112.5^{0} & .35\angle -22.5^{0} & .35\angle -135^{0} & .35\angle -45^{0} \\
0 & 0 & 0 & 0 & 0 & 0 & 0 & 0 & .35\angle -67.5^{0} & .35\angle 22.5^{0} & .35\angle 0^{0} & .35\angle 90^{0} & .35\angle -22.5^{0} & .35\angle 67.5^{0} & .35\angle -45^{0} & .35\angle 45^{0} \\
0 & 0 & 0 & 0 & 0 & 0 & 0 & 0 & .35\angle -90^{0} & .35\angle -90^{0} & .35\angle -112.5^{0} & .35\angle -22.5^{0} & .35\angle 67.5^{0} & .35\angle 157.5^{0} & .35\angle 67.5^{0} & .35\angle 157.5^{0} \\
0 & 0 & 0 & 0 & 0 & 0 & 0 & 0 & .35\angle 180^{0} & .35\angle 112.5^{0} & .35\angle 22.5^{0} & .35\angle 67.5^{0} & .35\angle 157.5^{0} & .35\angle -112.5^{0} & .35\angle 112.5^{0} & .35\angle 202.9^{0} \\
.35\angle -157^{0} & .35\angle 112.5^{0} & .35\angle 45^{0} & .35\angle -45^{0} & .35\angle 22.5^{0} & .35\angle -67.5^{0} & .35\angle -90^{0} & .35\angle 180^{0} & 0 & 0 & 0 & 0 & 0 & 0 & 0 & 0 \\
.35\angle 112.5^{0} & .35\angle 22.5^{0} & .35\angle -45^{0} & .35\angle -139^{0} & .35\angle 112.5^{0} & .35\angle 22.5^{0} & .35\angle -90^{0} & .35\angle 112.5^{0} & 0 & 0 & 0 & 0 & 0 & 0 & 0 & 0 \\
.35\angle 45^{0} & .35\angle -22.5^{0} & .35\angle -22.5^{0} & .35\angle -229^{0} & .35\angle -90^{0} & .35\angle 0^{0} & .35\angle 112.5^{0} & .35\angle 22.5^{0} & 0 & 0 & 0 & 0 & 0 & 0 & 0 & 0 \\
.35\angle 45^{0} & .35\angle -135^{0} & .35\angle -112.5^{0} & .35\angle -22.5^{0} & .35\angle 0^{0} & .35\angle 90^{0} & .35\angle -22.5^{0} & .35\angle 67.5^{0} & 0 & 0 & 0 & 0 & 0 & 0 & 0 & 0 \\
.35\angle 112.5^{0} & .35\angle -22.5^{0} & .35\angle 90^{0} & .35\angle -0^{0} & .35\angle 112.5^{0} & .35\angle -22.5^{0} & .35\angle 67.5^{0} & .35\angle 157.5^{0} & 0 & 0 & 0 & 0 & 0 & 0 & 0 & 0 \\
.35\angle 22.5^{0} & .35\angle -112.5^{0} & .35\angle 0^{0} & .35\angle -90^{0} & .35\angle -22.5^{0} & .35\angle 67.5^{0} & .35\angle 157.5^{0} & .35\angle -112.5^{0} & 0 & 0 & 0 & 0 & 0 & 0 & 0 & 0 \\
.35\angle -90^{0} & .35\angle 0^{0} & .35\angle -22.5^{0} & .35\angle 112.5^{0} & .35\angle -135^{0} & .35\angle -45^{0} & .35\angle 67.5^{0} & .35\angle 112.5^{0} & 0 & 0 & 0 & 0 & 0 & 0 & 0 & 0 \\
.35\angle 0^{0} & .35\angle -90^{0} & .35\angle -292.5^{0} & .35\angle 22.5^{0} & .35\angle -45^{0} & .35\angle 45^{0} & .35\angle 157.5^{0} & .35\angle 202.9^{0} & 0 & 0 & 0 & 0 & 0 & 0 & 0 & 0
\end{array}\right]$$

- The Signal flow for 8x8 Butler matrix with Rectangular Parallelepiped shaped patch antennas

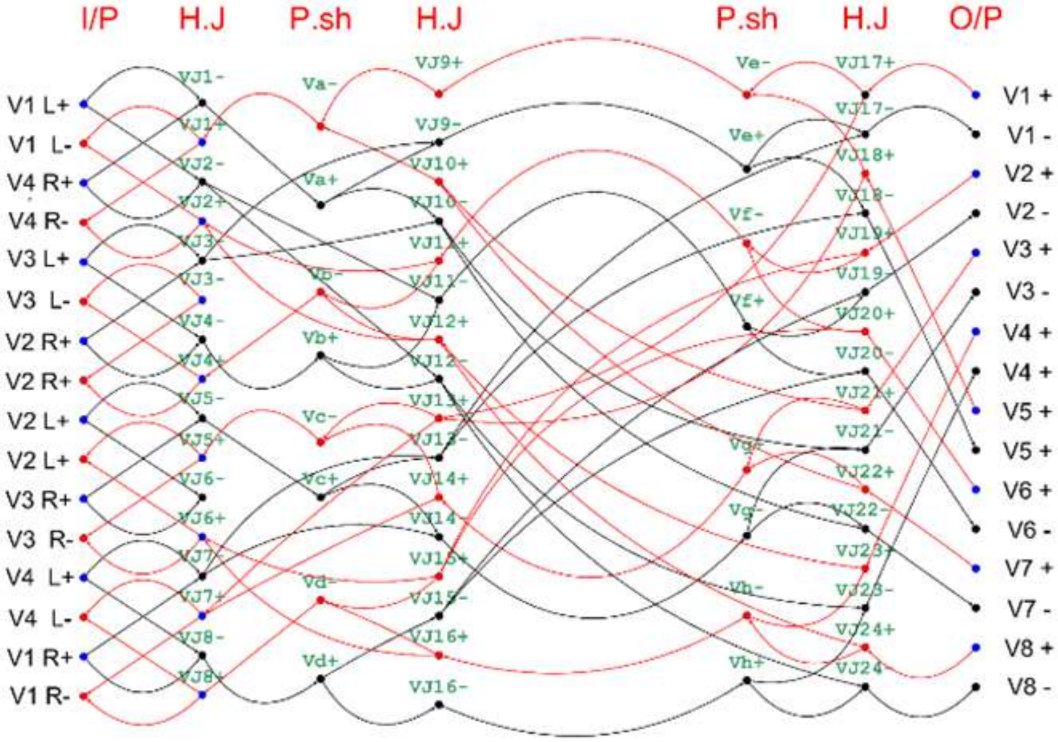

Table 3.5 Substrate Parameters

Substrate	Liquid Crystal
Dielectric Constant □ r	3.2
Substrate Height	m

3.2.1 <u>1st Trail</u> " 8x8 Butler Matrix with Rectangular Parallelepiped Shaped Patch Antennas "

The 8x8 Butler matrix with Rectangular Parallelepiped shaped patch antennas has been designed, simulated and optimized as shown in figure 3.5. While its simulated frequency response is shown in figure 3.6.

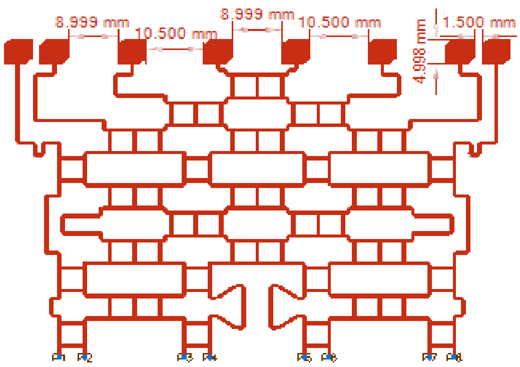

Figure 3.13 8x8 Butler Matrix with Rectangular Patch Antenna

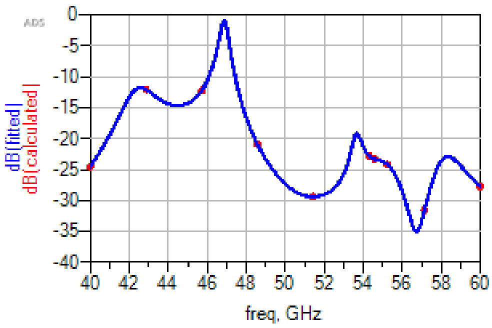

Figure 3.14 Shows the Return Loss of 8x8 Butler Matrix with Rectangular Patch Antenna

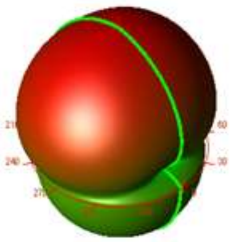

Figure 3.15 3D Radiation pattern of the 8x8 Butler matrix with Rectangular Parallelepiped Shaped Patch Antennas

TABLE 3.6 Antenna Parameters of the 8x8 Butler matrix with Rectangular Parallelepiped Shaped Patch Antennas

Antenna Parameters

Frequency (GHz)		35
Input power (Watts)		0.00834012
Radiated power (Watts)		0.00834012
Directivity(dBi)		15.0619
Gain (dBi)		15.0619
Radiation efficiency (%)		100
Maximum intensity (Watts/Steradian)		0.0212889
Effective angle (Steradians)		0.391758
Angle of U Max (theta, phi)	57	89
E(theta) max (mag,phase)	3.98719	-154.618
E(phi) max (mag,phase)	0.377771	-143.255
E(x) max (mag,phase)	0.340639	38.0011
E(y) max (mag,phase)	2.17771	-154.584
E(z) max (mag,phase)	3.34394	25.3817

OK

3.2.2 <u>2nd Trial</u> "8x8 Butler Matrix with Rectangular-cut at the Corners Shaped Patch Antennas with Slot"

Figure 3.16 Shows the rectangular patch antennas with cut at the corners with slots to generate circular polarized radiation pattern.

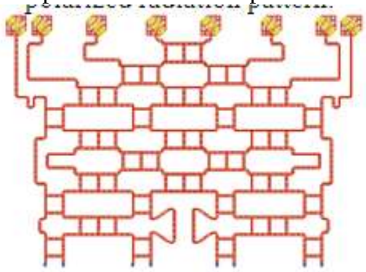

Figure 3.16 8x8 Butler Matrix with Rectangular Parallelepiped Shaped Patch Antennas with Slot

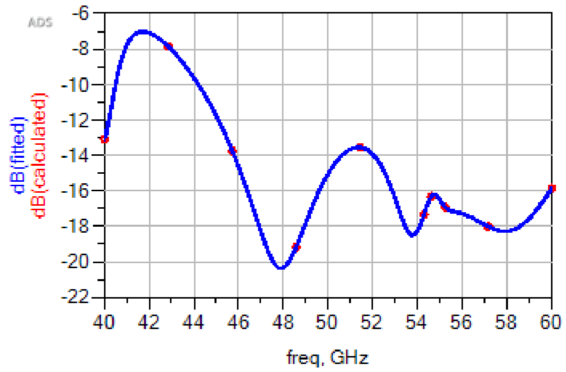

Figure 3.17 Shows the Return Loss of 8x8 Butler Matrix with Rectangular Parallelepiped Patch Antenna with Slot

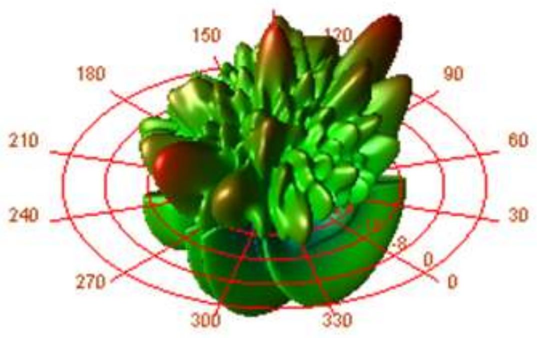

Figure 3.18 3D Radiation pattern of the 8x8 Butler Matrix with Rectangular Parallelepiped Shaped Patch Antenna with Slot

Table 3.7 Antenna Parameters of 8x8 Butler Matrix with Rectangular Parallelepiped Shaped Patch Antenna with Slot

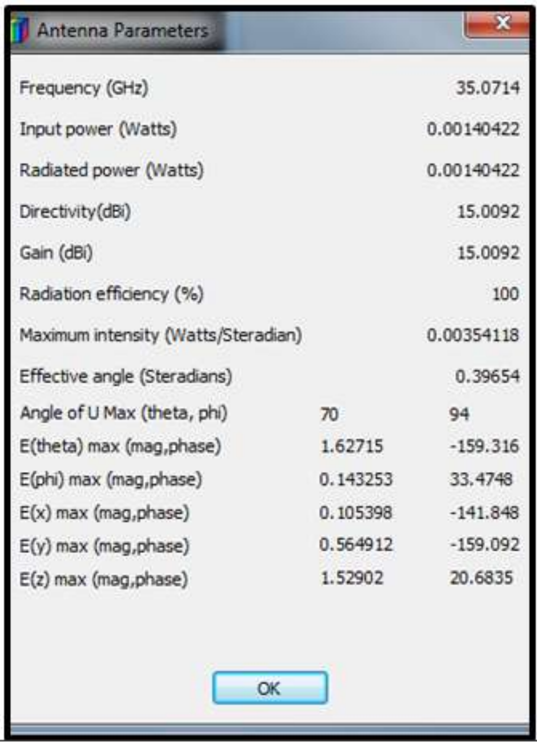

Antenna Parameters

Frequency (GHz)		35.0714
Input power (Watts)		0.00140422
Radiated power (Watts)		0.00140422
Directivity(dBi)		15.0092
Gain (dBi)		15.0092
Radiation efficiency (%)		100
Maximum intensity (Watts/Steradian)		0.00354118
Effective angle (Steradians)		0.39654
Angle of U Max (theta, phi)	70	94
E(theta) max (mag,phase)	1.62715	-159.316
E(phi) max (mag,phase)	0.143253	33.4748
E(x) max (mag,phase)	0.105398	-141.848
E(y) max (mag,phase)	0.564912	-159.092
E(z) max (mag,phase)	1.52902	20.6835

OK

3.2.3 <u>The Final Trail (The required Improved shape)</u> " 8x8 Butler Matrix with Rectangular-cut at the Corners Shaped Patch Antennas with Slot and Enhancement Factor "

Figure 3.19 Shows the rectangular patch antennas with cut at the corners with slots to generate circular polarized radiation pattern. Enhancement factor have been made in order to improve the performance this proposed 8x8 Butler matrix. Figure 3.20 show that the butler matrix network provides ultra-wideband (bandwidth) of greater than 20 GHz. The simulated gain of the matrix 8x8 given in figure 3.19 Gain 17.15 dB has been achieved see table 3.8. Figure 3.21 shows 3D radiation pattern of the proposed butler matrix.

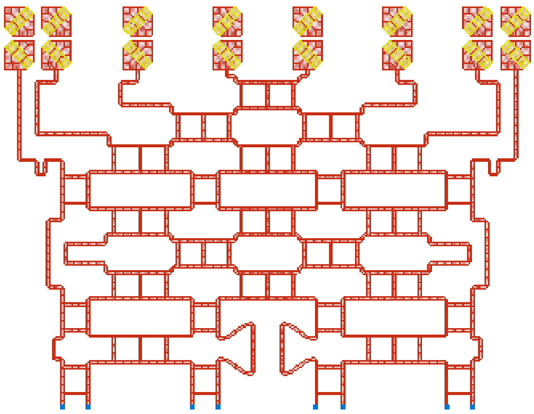

Figure 3.19 8x8 Butler matrix with Rectangular Parallelepiped shaped patch antennas with Slot and Enhancement Factor

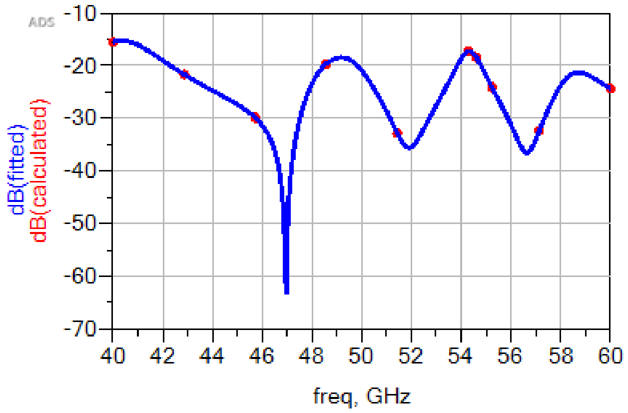

Figure 3.20 Shows the Return Loss of the 8x8 Butler matrix with Rectangular Parallelepiped Shaped Patch antenna with Slot and Enhancement Factor

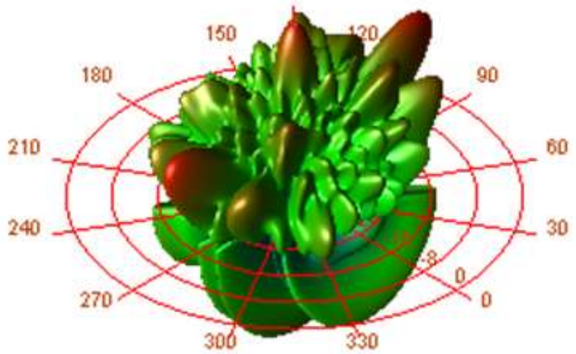

Figure 3.21 3D Radiation pattern of the 8x8 Butler Matrix with Rectangular Parallelepiped Shaped Patch Antenna with Slot and Enhancement Factor

Table 3.8 3 Antenna Parameters of 8x8 Butler Matrix with Rectangular Parallelepiped Shaped Patch Antenna with Slot and Enhancement Factor

Antenna Parameters

Power radiated (Watts)		0.0400509
Effective angle (Steradians)		0.240529
Directivity(dBi)		17.1804
Gain (dBi)		17.1575
Maximim intensity (Watts/Steradian)		0.166511
Angle of U Max (theta, phi)	56	90
E(theta) max (mag,phase)	11.1922	-20.8078
E(phi) max (mag,phase)	0.441497	1.99019
E(x) max (mag,phase)	0.441497	-178.01
E(y) max (mag,phase)	6.25859	-20.8078
E(z) max (mag,phase)	9.27873	159.192

OK

❖ It is clear from figure 3.21 that the 3D radiation pattern obtained is acceptable according to the design requirement which required circular polarized operation.

IV. Conclusion

The individual components which form both 4×4 and 8×8 butler matrices are improved successively with broadband operations. Unique signal flows for the single elements which are composing the proposed butler matrices (the one-section and two-sections branch line couplers) are developed.

This improvements in the individual components have led to overall improvements in the performances 4×4 and 8×8 butler matrices. This signal flow for both 4×4 and 8×8 butler matrices are derived successively at the central frequency.

The most suitable microstrip selected patch antenna to produce the required performances on 4×4 and 8×8 butler matrices. The selected liquid crystal substrate for the high frequency operation is utilized in order to achieve ultra-broadband operations. A bandwidth of greater than 20 GHz is observed.

Appendix A

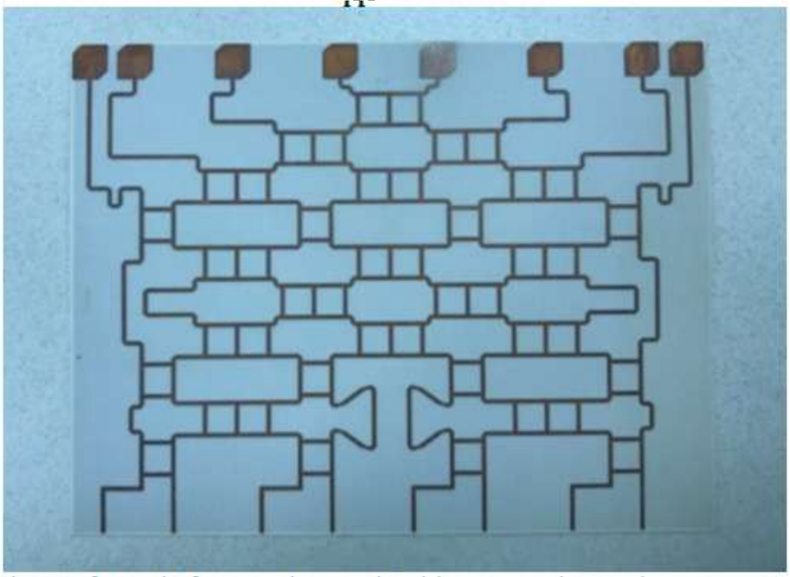

Figure A-1: Typical Manufactural of 8x8 Butler Matrix with Rectangular Patch Antenna on Roger substrate for further work

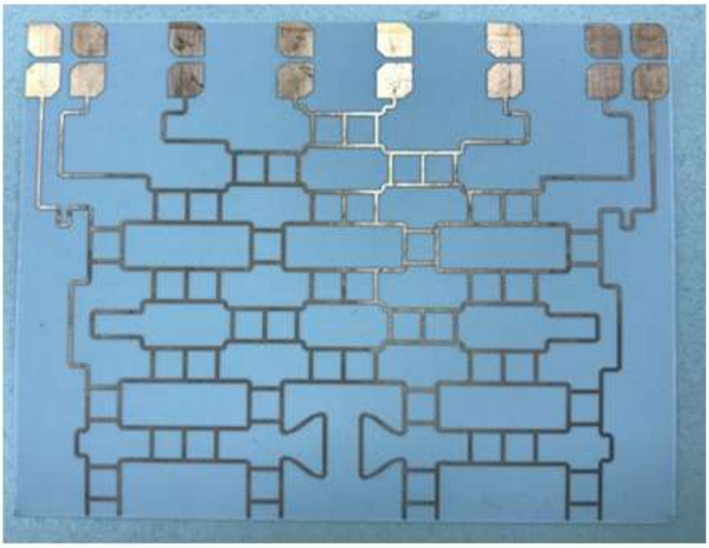

Figure A-2: Typical Manufactural 8x8 Butler matrix with Rectangular Parallelepiped shaped patch antennas with Enhancement Factor on Roger substrate for further work

References

[1]. J. Butler and R. Lowe, “Beam forming matrix simplifies design of electronically scanned antennas,” Electron. Design, vol. 9, pp. 170–173, Apr. 1961.
[2]. Y. S. Wong, S. Y. Zheng, and W. S. Chan, “Quasiarbitrary phase-difference hybrid coupler,” IEEE Trans. Microw. Theory Tech., vol. 60, no. 6, pp. 1530-1539, Jun. 2012.
[3]. K. J. Ding, X. X. Fang, Y. Z. Wang, and A. X. Chen, “Printed Dual-Layer Three-Way Directional Coupler Utilized as 3×3 Beamforming Network for Orthogonal Three-Beam Antenna Array,” Antennas Wireless Propag. Lett. vol. 13, 2014, pp. 911-914. May. 2014.
[4]. L. G. Sodin, “Method of synthesizing a beam-forming device for the N-beam and N-element array antenna, for any N,” IEEE Trans. Antennas Propag., vol. 60, no. 4, pp. 1771–1776, Apr. 2012.
[5]. Djerafi, T., N. J. G. Fonseca, and K. Wu, “Design and implementation of a planar 4 × 4 Butler matrix in SIW technology for wide band high power applications,” Progress In Electromagnetics Research B, Vol. 35, 29–51, Oct. 2011.
[6]. Chen, C.-J. and T.-H. Chu, “Design of a 60-GHz substrate integrated waveguide Butler matrix-a systematic approach,” IEEE Transactions on Microwave Theory and Techniques, Vol. 58, No. 07, 1724–1733, Jul. 2010.
[7]. Mohamed Ali, A. A., N. J. G. Fonseca, F. Coccetti, and H. Aubert, “Design and implementation of two-layer compact wideband Butler matrices in SIW technology for Ku-band applications,” IEEE Transactions on Antennas and Propagation, Vol. 59, No. 02, 503–512, Feb. 2011.
[8]. Cheng, Y. J., C. A. Zhang, and Y. Fan, “Miniaturized multilayer folded substrate integrated waveguide Butler matrix,” Progress In Electromagnetics Research C, Vol. 21, 45–58, Apr. 2011.
[9]. Ahmad, S. R. and F. C. Seman, “4-port Butler matrix for switched multibeam antenna array,” APACE’05, Johor, Malaysia, Dec. 20–21, 2005.
[10]. Dominguez, G. E., J.-M. Fernandez-Gonzalez, P. Padilla, and M. Sierra-Castafier, “Mutual coupling reduction using EBG in steering antennas,” IEEE Antennas and Wireless Propagation Letters, Vol. 11, 1265

Abdullah H. Alhazmi "Ultra-broadband 4×4 and 8×8 Butler Beam Forming Networks on Liquid Crystal Substrate at 51Ghz" International Refereed Journal of Engineering and Science (IRJES), vol. 07, no. 06, 2018, pp. 45-62